Author Manuscript Published OnlineFirst on July 30, 2019; DOI: 10.1158/0008-5472.CAN-19-0698
Author manuscripts have been peer reviewed and accepted for publication but have not yet been edited.

MEK inhibition modulates cytokine response to mediate therapeutic efficacy in lung cancer

Running title: Cytokine response modulatory function of MEK inhibitors

Mengyu Xie[1,2], Hong Zheng[1], Ranjna Madan-Lala[1], Wenjie Dai[1], Nicholas T. Gimbrone[2,3], Zhihua Chen[4], Fumi Kinose[5],Sarah A. Blackstone[1], Keiran S. M. Smalley[6] ,W. Douglas Cress[3,5], Eric B. Haura[5], Uwe Rix[5, 7] and Amer A. Beg[1,5]

Conflicts of interest: The authors declare no potential conflicts of interest.

[1]Department of Immunology, Moffitt Cancer Center, Tampa, FL 33612, USA. [2]Cancer Biology PhD Program, University of South Florida, Tampa, FL 33612, USA. Departments of [3]Molecular Oncology, [4]Bioinformatics, [5]Thoracic Oncology, [6]Tumor Biology, [7]Drug Discovery, Moffitt Cancer Center, Tampa, FL 33612, USA.

Correspondence should be addressed to A.A.B at Moffitt Cancer Center, 12902 Magnolia Drive, SRB-2, Tampa Florida 33612. Phone: 813-745-5714. Email: amer.beg@moffitt.org

Abstract

Activating mutations in BRAF, a key mediator of RAS signaling, are present in ~50% of melanoma patients. Pharmacological inhibition of BRAF or the downstream MAP kinase MEK are highly effective in treating BRAF-mutant melanoma. In contrast, RAS pathway inhibitors have been less effective in treating epithelial malignancies, such as lung cancer. Here, we show that treatment of melanoma patients with BRAF and MEK inhibitors (MEKi) activated tumor NF-κB activity. MEKi potentiated the response to TNFα, a potent activator of NF-κB. In both melanoma and lung cancer cells, MEKi increased cell surface expression of TNFα receptor 1 (TNFR1), which enhanced NF-κB activation and augmented expression of genes regulated by TNFα and IFNγ. Screening of 289 targeted agents for the ability to increase TNFα and IFNγ target gene expression demonstrated that this was a general activity of inhibitors of MEK and ERK kinases. Treatment with MEKi led to acquisition of a novel vulnerability to TNFα and IFNγ-induced apoptosis in lung cancer cells that were refractory to MEKi killing and augmented cell cycle arrest. Abolishing the expression of TNFR1 on lung cancer cells impaired the anti-tumor efficacy of MEKi while the administration of TNFα and IFNγ in MEKi-treated mice enhanced the anti-tumor response. Furthermore, immunotherapeutics known to induce expression of these cytokines synergized with MEKi in eradicating tumors. These findings define a novel cytokine response modulatory function of MEKi which can be therapeutically exploited.

Significance

Lung cancer cells are rendered sensitive to MEK inhibitors by TNFα and IFNγ, providing strong mechanistic rationale for combining immunotherapeutics, such as checkpoint blockers, with MEK inhibitor therapy for lung cancer.

Introduction

Activating mutations in the RAS pathway comprise one of the most common oncogenic abnormalities in cancer. Mutations in the RAS effector BRAF kinase are present in approximately half of all melanoma patients. Pharmacological targeting of BRAF and the downstream MEK-ERK kinases results in significant benefit in *BRAF* mutant melanoma patients (1, 2). This vulnerability is due to addiction of *BRAF* mutant melanoma to the BRAF-MEK pathway (1, 3). RAS pathway mutations are also common in epithelial tumors, e.g. ~30% of lung adenocarcinoma patients have mutations in *KRAS*. Unlike *BRAF* mutant melanoma, RAS pathway inhibitors, such as MEK inhibitors (MEKi), have shown limited efficacy in lung cancer treatment (2, 4). This is likely because *KRAS* mutations are not always associated with KRAS pathway addiction (5, 6) as well as the redundancy in the function of downstream effector pathways for cancer cell survival e.g. MEK and PI3K pathways (7-10). New strategies therefore need to be developed for treating *KRAS* mutant cancers.

A variety of approaches are being pursued to target the RAS pathway including the development of inhibitors that directly target RAS proteins (10). An approach that has been pursued for some time is the simultaneous targeting of multiple arms of the RAS pathway, such as PI3K-AKT and MEK-ERK (8). However, there is concern about the toxicity of combinations of inhibitors of these pathways (2). Immunotherapeutics, especially those targeting checkpoint receptors on T cells, have revolutionized treatment of many cancer types. Interestingly, analysis of melanoma patient biopsies after BRAF and MEK inhibitor treatment indicate increased presence of tumor infiltrating lymphocytes (TILs) (11-13). Since patient benefit from immunotherapy is associated with high tumor expression of immune surveillance genes and T cell infiltration (14-16), it has been proposed that MEKi may help generate a tumor microenvironment that enhances response to immunotherapy (17-20). Indeed, combining MEKi with immunotherapy (e.g. T cell checkpoint blockade) in the pre-clinical setting substantially

improved efficacy (17-20). Therefore, MEKi may find use in combination with immunotherapies in tumor types that are otherwise resistant to MEKi.

In previous studies we found that NF-κB regulates tumor immune surveillance (21). We hypothesized that MEKi may activate NF-κB to generate a tumor microenvironment that is more permissive to immunotherapy. In both human tumors and in established cell lines, we show that MEKi enhances expression of NF-κB target genes. This was mediated by MEKi induced upregulation of cell surface expression of TNFR1 which strongly potentiated gene expression responses by TNFα as well as genes jointly regulated by TNFα and IFNγ. Furthermore, MEKi cooperated with PD-1 blockade immunotherapy in curtailing lung tumor growth. A key and unexpected finding was the synergy between MEKi and TNFα + IFNγ in inducing cancer cell growth arrest and apoptosis across a broad array of human and mouse lung cancer cell lines. Furthermore, cancer cell knockout of TNFR1 impaired the anti-tumor activity of MEKi. Such cross-talk between MEKi and cytokine signaling pathways indicates a novel mechanism of action for an anti-cancer agent which could be used to enhance therapeutic efficacy against cancer types that are minimally responsive to MEKi.

METHODS

Cell lines

Lung cancer and melanoma cell lines were provided by the Moffitt Lung Cancer Center of Excellence Cell Line Core and Dr. Keiran Smalley, respectively. Cell lines tested negative for mycoplasma contamination (PlasmoTest, Mycoplasma Detection Kit from InvivoGen, San Diego, CA) and have been authenticated by STR analysis. All lung cancer and melanoma cell lines were maintained in RPMI 1640 with 10% fetal bovine serum and passaged for 2-4 times before use in experiments. NIH-3T3 cells were obtained from ATCC and maintained in DMEM with 10% fetal bovine serum. All cells were cultured with 10% fetal calf serum at 37 degrees in a 95% air, 5% CO2 humidified incubator.

Drug library screening for CCL5 and CXCL10 expression

The COCTAIL library of 289 different agents was plated on cultures of A549 cells in 96 well plates (10,000 cells/well) using the Biotek robotic system. 24 hrs later, 2 different concentrations of each drug was added: 0.1 μM and 1 μM. TNFα and IFNγ were added to final concentrations of 0.2 ng/ml and 1 ng/ml, respectively. All conditions were in duplicate and the average was used in **Fig. 2B**. Cell supernatants were removed to determine amounts of secreted chemokines CCL5 and CXCL10 24hrs later. Cell viability was also determined using the CellTiter-Glo® Reagent. Chemokine levels in A549 supernatant were detected using Bead-Based Multiplex Assays (Millipore Inc.) with Luminex technology.

Mice

All mice were bred and housed in the animal facility at Moffitt Cancer Center under specific pathogen-free conditions. 129S4/SvJaeJ mice were originally obtained from Jackson laboratory

and were used for LKR tumor studies. Immunodeficient SCID mice (CB17.Cg-Prkdc^{scid}Lyst^{bg-J}/Crl) were purchased from Charles River and used for A546 tumor growth studies. All animal experiments were approved by the Institutional Animal Care and Use Committee.

Flow cytometric analysis

Cells were incubated for 5 minutes at room temperature with Fc block (BD Biosciences). Staining was performed in 1% BSA/PBS for 15 min at room temperature with Fluorochrome-conjugate monoclonal antibodies, and DAPI was added prior to analysis to assess viability. Flow cytometric analysis was performed on an LSR II cytometer (BD Biosciences). Data were acquired using FACSDiva software (BD Biosciences) and analyzed using FlowJo software (Tree Star). The antibodies used from Miltenyi Biotec were CD120a (TNF-R1)-APC, human (clone: REA252); CD120b (TNFαRII)-PE, human (clone: REA520). PE anti-mouse CD120a (TNFαR Type I/p55) antibody was from Biolegend.

CRISPR/Cas9 gene knockout

Human TNFR1CRISPR/Cas9 knockout plasmids were purchased from Santa Cruz Biotechnology. Specifically, cells were kept 40–80% confluency in a 6 cm plate, and replaced with fresh antibiotic-free growth medium prior to transfection. 1 µg of plasmid DNA was incubated in 25ul FuGENE Transfection Reagent (Promega) for 5 minutes and then added to 200ul serum-free opti-MEM for less than 20 minutes. After 72 hours of transfection, green fluorescent protein – positive (GFP+) cells were single-cell sorted into 96-well plates. Single clones were then expanded and screened by flow cytometry and western blot analysis of TNFR1 expression.

Subcutaneous tumor studies

Cells were harvested in logarithmic growth phase after being cultured for less than 2 weeks, washed once in injection medium (phenol-free DMEM supplemented with 2% FBS) and counted. Cells were injected subcutaneously into the right flank of mice and measured every 4 days. For LKR tumors, 10^6 LKR cells were injected in phenol-free DMEM injection medium. The tumor volume was determined as length x length x width/2. Trametinib (1mg/kg or 3mg/kg) or vehicle was oral gavaged daily, αPD-1 (Clone RMP1-14) or isotype control (Bio-X-Cell) was injected intraperitoneally (250 μg/mouse per injection). To deplete T cells, 300 μg/mouse anti-mCD4 (Clone GK1.5), mCD8 (Clone 2.43) or isotype control (Bio-X-Cell) were injected intraperitoneally one day prior to anti-tumor treatment and repeated every 3 days until experiment end point. For intratumoral cytokine injection, 100μl of TNFα and IFNγ (0.5μg each) or 100μl PBS were injected directly into the tumor tissue for 3 consecutive days (day 11 to day 13 post tumor cell inoculation), trametinib dosing was from day 10 to day 14.. Mice were sacrificed at the end of experiment or when tumor volume exceeded 2,000 mm^3.

Orthotopic tumor studies and bioluminescence imaging

2.5 $x10^5$ A549 cells were injected with PBS plus 1:1 volume Matrigel (Corning) percutaneously into the left lateral thorax in mice anesthetized with isoflurane. 14 days later later, trametinib (1mg/kg) or vehicle was oral gavaged daily for 14 days and tumors were monitored using live imaging system. At the end of the study, lungs were collected for histological analysis. For bioluminescence imaging (BLI), firefly luciferase-expressing A549 or LKR were used. The IVIS Imaging system was used to capture bioluminescence following i.p. injection of 4 mg luciferin (Gold Biotechnology).

Statistical analysis

For two group comparisons, Student's t-test or paired t-test (two-sided) was applied. In time course experiments that involve repetitive measurements, two-way ANOVA was applied to

determine group differences and *post hoc* multiple-comparisons (Sidak's or Tukey's method, see below) were applied to individual time points. Significance for multiple condition experiments was determined using one-way ANOVA. For type I corrections for multiple-comparisons, Sidak's method was applied for comparisons between specific pairs of conditions, Tukey's method was applied for pair-wise comparisons among all conditions. For *in vivo* experiments, Dunnett's method was adopted to compare each treatment group with the control group. Correlations between two numerical metrics were determined using Pearson's r. Cell cycle data of each individual experiment was represented using a contingency table, chi-squared test with Bonferroni correction was applied to determine the significance. Differences between tumor growth curves were determined by two-way ANOVA. In the figures, significance was noted using *$p < 0.05$, **$p < 0.01$, ***$p < 0.001$,****$p < 0.0001$, ns, not significant. All data shown in the bar graphs are the mean ± SD of at least three biological replicates. Statistical analysis was conducted using the Prism7 (GraphPad) software.

Results

MEK inhibitors enhance TNFα induced gene expression

Inhibitors of BRAF (BRAFi e.g. dabrafenib) and MEK (e.g. trametinib) prevent ERK activation and are the standard-of-care for treatment of *BRAF* mutant melanoma. To determine whether BRAFi/MEKi impacts NF-κB signaling, we used RNA-sequencing data from pre-treatment and on-treatment biopsies of patients in a recent study (22). We used an NF-κB gene expression signature (21) to determine potential changes in NF-κB activity after BRAFi/MEKi treatment. Importantly, NF-κB pathway activity was significantly enhanced after treatment (**Fig. 1A**). Importantly, on-treatment NF-κB activity was significantly associated with depth of patient response to treatment (**Fig. 1B**). TNFα is a master activator of NF-κB, including in the tumor microenvironment, and previous studies have shown increased TNFα levels in melanoma patients undergoing BRAFi treatment (23-25). We hypothesized that MEKi may increase TNFα expression and/or TNFα induced NF-κB activation leading to elevated target gene expression. We tested this in vitro by using *BRAF* mutant WM164 and 1205Lu human melanoma cell-lines to determine changes in mRNA expression of *TNF* and the TNFα target gene *TNFAIP3* (aka A20). Consistent with previously established autocrine regulation of TNFα, we found that TNFα enhanced expression of *TNF* in addition to *TNFAIP3*. Notably, MEKi trametinib enhanced TNFα-induced expression of both genes in these melanoma cell-lines (**Fig. 1C, D**). These results suggest that MEKi potentiates TNFα signaling in melanoma cells, which may be linked to enhancement of NF-κB activity after BRAFi/MEKi treatment.

Unlike melanoma, MEKi have shown limited efficacy in lung cancer treatment (2, 4). With the goal of defining strategies to increase vulnerability of lung cancer to MEKi, we next determined whether a similar potentiation of TNFα induced gene expression by MEKi was evident in lung

cancer cells. To broadly assess such a role for MEKi, we performed exome-wide gene expression studies in the *KRAS* mutant human lung adenocarcinoma cell-line A549. Interestingly, MEKi trametinib slightly enhanced expression of several TNFα target genes, including *TNF* and *TNFAIP3*, but the highest levels of expression were achieved after combined MEKi and TNFα treatment (**Fig. 1E and Table S1**). qRT-PCR confirmed ability of MEKi to enhance expression of *TNF* and *TNFAIP3* in A549 and when combined with TNFα (**Fig. 1F)** and in the H2122 lung cancer cell-line (**Fig. S1**). TNFα and IFNγ synergize in regulating expression of a host of immune function genes, such as the chemokine *CXCL10,* which was found to be upregulated by TNFα + MEKi (**Fig. 1E)**. TNFα + IFNγ synergistically enhanced *CXCL10* expression which was further enhanced in the presence of MEKi (**Fig. 1G)**. The same results were obtained when expression levels of CXCL10 protein were determined (**Fig. 1H)**.

MEK and ERK inhibitors stimulate TNFα + IFNγ induced chemokine expression

We next determined whether MEKi stimulation of TNFα induced gene expression also occurred in response to other anti-cancer agents. We assembled an in-house customized library of 289 targeted compounds that cover all major target classes, such as epigenetic enzymes, hedgehog, HSP90 and Notch, but has a stronger focus on protein and lipid kinases that reflects the current landscape of targeted agents in clinical use and development (26). This library consists of more than 70% of compounds that are either FDA approved or in clinical development (thus the name COCTAIL - Collection of Clinical Targeted Agents In Lung cancer) (**Fig. S2 and Table S2**). In addition, we incorporated target redundancy so that most targets are covered by several compounds. Both CXCL10 and CCL5 are synergistically regulated by TNFα + IFNγ. We used this library to identify anti-cancer agents that can enhance TNFα + IFNγ induced expression of CXCL10 and CCL5 in A549. The combination of TNFα + IFNγ was used

based on the reasoning that agents capable of enhancing the already high expression induced by these cytokines will yield the most robust hits. Using the basic scheme outlined in **Fig. 2A**, we determined ability of two different concentrations (0.1 and 1μM) of each of these agents to increase TNFα + IFNγ induced secretion of CXCL10 and CCL5 (**Table S2**). Using a 2-fold cut-off for ability to increase expression in one of the 4 tested conditions over TNFα + IFNγ alone, 16 agents were identified as potential hits. Remarkably, 13 of these agents were either MEK (including trametinib) or ERK inhibitors (**Fig. 2B**). The additional agents included 2 SMAC mimetics, which target cIAP proteins and activate TNFα signaling (27), and a phosphodiesterase inhibitor (**Fig. 2B**). We conclude the MEK/ERK inhibitors can function to enhance TNFα + IFNγ induced signaling responses. Furthermore, the multitude of MEK/ERK inhibitors identified suggest that on-target effects of these drugs are responsible for enhancement of TNFα + IFNγ induced responses.

MEKi enhance cell surface expression of TNFα receptor 1

To investigate how TNFα and TNFα + IFNγ gene expression responses might be enhanced by MEKi, we next determined its impact on the expression of the two TNFα receptors: TNFR1 and TNFR2. Interestingly, MEKi led to dramatic cell surface upregulation of TNFR1, but not TNFR2, in a dose-dependent manner in A549 (**Fig. 3A-C)**. However, the total levels of TNFR1 were not impacted (**Fig. 3C)** suggesting that MEKi increases membrane localization of TNFR1. TNFα treatment itself did not enhance TNFR1 expression (**Fig. 3A, B)**. In contrast to MEKi, cytotoxic agents and drugs targeting PI3K or HDACs failed to upregulate TNFR1 expression (**Fig. S3A**). We next determined whether MEKi induced increase in TNFR1 impacted NF-κB activation by TNFα and IFNγ as determined by RelA phosphorylation and increase in nuclear translocation of RelA. MEKi alone activated NF-κB and its target genes *TNF* and *TNFAIP3* in A549 (**Fig. S3B-**

C), but in combination with TNFα NF-κB activation was synergistically enhanced (**Fig. 3D**). Interestingly, the combination of MEKi + IFNγ also enhanced NF-κB activation suggesting that MEKi enhancement of TNFR1 expression may also potentiate IFNγ responses (**Fig. 3D**). Finally, the highest activation of NF-κB was seen in the presence of MEKi and both cytokines.

MEKi also increased TNFR1 surface expression in multiple additional human lung cell-lines such as H2122, H1437, HCC44 and PC9 (**Fig. 3E**) and the *BRAF* mutant WM164 and 1205Lu human melanoma cell-lines by both MEKi and BRAFi (**Fig. S3D**). TNFR1 upregulation was seen in both *KRAS* mutant (A549, H2122, HCC44, H2009) and wild-type (H1437, PC9) human lung cancer cell-lines (**Fig. 3E**). We believe this likely reflects the common utilization of MEK-ERK signaling by cancer cells regardless of oncogene mutation. Similar results were also obtained in mouse lung cancer LKR which harbors *Kras* mutation (**Fig. 3E**). We next tested 3 additional MEKi included in the above screening (cobimetinib, binimetinib/MEK162 and AZD8330) for their ability to inhibit pERK, upregulate TNFR1 expression and induce gene expression (**Fig.S4A-C**). In a dose-dependent manner, these MEKi inhibited pERK and upregulated cell surface TNFR1 but not TNFR2 expression (**Fig.S4A-B**). Moreover, as observed in **Fig. 3C** for trametinib, these MEKi did not impact total TNFR1 levels (**Fig.S4A**). Importantly, we found a strong association between pERK inhibition and surface expression of TNFR1 and target gene expression (**Fig. S4D-F**). As seen with trametinib, these MEKi also enhanced TNFα induced *TNF* expression in a dose dependent manner (**Fig.S4C**). Furthermore, *TNF* expression strongly correlated with pERK inhibition (**Fig.S4E**) and surface expression of TNFR1 (**Fig.S4F**). We determined whether enhanced activation of MEK/ERK could conversely reduce TNFR1 expression. Importantly, ectopic expression of mutant KRAS in NIH-3T3 fibroblasts enhanced ERK activation and reduced cell surface TNFR1 expression **Fig. 3F, G**). These results indicate ability of MEKi to enhance surface expression of TNFR1, which in turn may be responsible for enhancement of TNFα-induced gene expression responses.

To determine the role in MEKi-induced stimulation of gene expression responses, TNFR1 was knocked-out (KO) in A549 using CRISPR/Cas9 technology. TNFR1 absence was confirmed by flow cytometry and western blotting (**Fig. S5A, B**), consistent with which TNFα induced gene expression was diminished in TNFR1 KO A549 (**Fig. S5C**). To determine impact of TNFR1 absence on TNFα and IFNγ gene expression responses, we assessed impact on *CXCL10* as it is dually regulated by both cytokines (**Fig. 1G)**. The absence of TNFR1 significantly reduced IFNγ and MEKi + IFNγ induced *CXCL10* expression, which was rescued by TNFR1 re-expression (**Fig. 3H**). Thus, TNFR1 mediates responses to IFNγ + MEKi likely through MEKi upregulation of TNFα-TNFR1 autocrine signaling which synergized with IFNγ. TNFα alone did not appreciably induce *CXCL10* but a notable increase was seen when TNFα was combined with MEKi. TNFα + IFNγ induced high level *CXCL10* expression which was further enhanced by MEKi in TNFR1 dependent manner (**Fig. 3H**). These results suggest that upregulation of TNFR1 by MEKi plays a key role in enhancing TNFα and IFNγ target gene expression. To test whether MEKi may also directly impact the IFNγ pathway, we determined cell surface IFNγ receptor 1 and 2 expression, which together make the IFNγ receptor heterodimer, as well as IFNγ induced STAT1 phosphorylation in the presence of MEKi (**Fig. S5D-G**). Unlike TNFR1, we did not see an increase in either IFNγ receptor chain expression (**Fig. S5D**). Furthermore, MEKi did not impact levels of IFNγ induced pSTAT1 across several IFNγ concentrations (**Fig. S5E**). At 0.5 and 5ng/ml IFNγ treatment at different time points, MEKi did not increase pSTAT1 levels but substantially increased IFNγ-induced *CXCL10* expression (**Fig. S5F-G**). We conclude that upregulation of both TNFα and IFNγ induced gene expression in A549 is mediated by MEKi induced increase in cell surface TNFR1.

TNFα and IFNγ modulate MEKi induced growth suppression and cell death

Author Manuscript Published OnlineFirst on July 30, 2019; DOI: 10.1158/0008-5472.CAN-19-0698
Author manuscripts have been peer reviewed and accepted for publication but have not yet been edited.

In addition to gene expression functions, TNFα is a known and potent inducer of cell death. Furthermore, TNFα and IFNγ synergize in induction of cell death and cell cycle arrest (28, 29). We next tested the possibility that MEKi induced increase in TNFR1 expression may also impact cell death and cell cycle arrest responses. Importantly, we observed that the growth suppressive effects of MEKi was partly attenuated in TNFR1 KO A549 but the re-expression of TNFR1 in these cells re-sensitized them to MEKi (**Fig. 4A**). These results suggest that activation of autocrine TNFR1/TNFα signaling by MEKi could enhance growth suppression. We next tested the impact of exogenous addition of TNFα and IFNγ. TNFα alone and TNFα + IFNγ were found to modestly reduce viable cell numbers. As expected, MEKi reduced cell numbers; however, the combination of MEKi with TNFα + IFNγ resulted in the most reduction in viable cell numbers (**Fig. 4B)**. Treatment with MEKi in the presence of both cytokines led to largest percentage of G1-phase cells and the lowest percentage S-phase cells (**Fig. 4C**) and the highest activation of apoptosis marker cleaved caspase 3 (**Fig. 4D**). These results suggest that reduction in viable cell numbers after MEKi and cytokine treatment are mediated through both cell cycle arrest and cell death induction (also see sections below).

Utilizing TNFR1 KO A549, we next tested the in vivo role of TNFR1 signaling in MEKi anti-tumor response in an orthotopic lung tumor model using immunodeficient SCID ($Prkdc^{scid}$) and beige ($Lyst^{bg}$) mice. Unlike vehicle treated mice, dosing of mice with 1mg/kg trametinib was associated with minimal tumor burden (**Fig. 4E, F**). In contrast, no reduction in tumor burden was noticed after MEKi treatment in mice bearing TNFR1 KO tumors (**Fig. 4E, F**). Importantly, pERK was strongly inhibited by MEKi in KO tumors suggesting that trametinib retains MEK targeting ability in these tumors (**Fig. 4G**). To longitudinally assess impact of MEKi on tumor growth, we utilized bioluminescence imaging (BLI) in parental and TNFR1 KO A549. While WT tumor growth was inhibited, TNFR1 KO tumors continued to grow after MEKi treatment **(Fig. S6A, B**). Together with in vitro findings, these results indicate a key role for TNFR1 signaling in

the MEKi anti-tumor response. Furthermore, since mouse TNFα cannot signal through human TNFR1, the anti-tumor effects of MEKi are likely mediated by stimulation of autocrine TNFα signaling.

We next tested the impact of TNFα and IFNγ on MEKi growth suppression in the mouse lung cancer LKR cell line, which also underwent increase in TNFR1 cell surface expression after MEKi treatment (**Fig. 3E**). As in A549 cells, the combination of MEKi with both TNFα and IFNγ led to the strongest reduction in cell numbers in LKR cells (**Fig. 5A**). However, individual cytokine treatment with IFNγ +MEKi decreased cell numbers while TNFα + MEKi treatment increased cell numbers compared to MEKi alone (**Fig. 5A**). To better understand these findings, we next proceeded to define the individual and combined roles of TNFα and IFNγ in LKR cell cycle and cell death regulation. However, TNFα + MEKi or TNFα + IFNγ + MEKi did not appreciably impact S-phase cells compared to MEKi alone (**Fig. 5B**). This was distinct from above results with A549 and suggests that decrease in LKR numbers after TNFα + IFNγ + MEKi (**Fig. 5A**) could be mediated by enhanced cell death.

To assess the role of apoptosis in reduction of viable cells after cytokine and MEKi treatments, we determined the levels of Cleaved Caspase 3 (CC3). CC3 comprises a 19kd (p19) and a 17kd (p17) fully activated form, both of which were detected in LKR cells. We found that in a dose dependent manner, TNFα promotes the formation of the p19 fragment and a small amount of p17 (**Fig. 5C**). This increase was not evident after either MEKi or IFNγ treatment (**Fig. 5C**). While the combination of TNFα or IFNγ with MEKi led to distinct and complex patterns of p19 and p17 activation, the combination of all 3 agents led to the highest level p17 activation (**Fig. 5C**). To determine the degree of enhancement of CC3 after the combination treatment, we treated LKR cells with 10nM MEKi and a range of cytokine concentrations (2, 10 and 50ng/ml). CC3 p17 generation was detected at the higher cytokine concentrations (10 and 50ng/ml)

consistent with reduction in viable cell numbers (**Fig. 5D**). However, CC3 p17 generation was dramatically enhanced at all 3 cytokine concentrations in the presence of MEKi (**Fig. 5D**) indicating that MEKi enhances sensitivity to cytokine induced apoptosis. Collectively, these results suggest that cell death induction rather than cell cycle arrest is the primary mechanism of cell number reduction in LKR cells after cytokine and MEKi treatment.

We next determined whether cytokine + MEKi effect on cell viability seen in vitro was also evident in vivo. A tumor stasis effect of MEKi was observed in sub-cutaneous (s.c.) LKR tumors at 1mg/kg and 3mg/kg daily dosing in an LKR (**Fig. S7**). Owing to similarity of response at these two concentrations, further studies were performed at the 1mg/kg dose. Consistent with in vitro results, upregulation of TNFR1 expression in tumor cells was also observed after MEKi treatment (**Fig. S8**). We next determined whether direct intratumoral injection of cytokines could impact the MEKi anti-tumor effect. BLI imaging of LKR tumors was used to determine treatment impact on tumor cell viability. Since TNFα + IFNγ have the potential to make tumor cells more susceptible to T cell killing, e.g. by upregulation of MHC expression, we specifically depleted T cells to better assess the tumor cell-intrinsic effects of cytokine treatment. Consistent with in vitro results, these results indicate that combining MEKi and cytokines results in the most significant loss of tumor cell viability (**Fig. 5E**). PD-1 blockade is a known inducer of IFNγ and TNFα secretion by T cells, including in the LKR model (30, 31). PD-1 blockade induced tumor regression in a subset of LKR tumor bearing mice (**Fig. 5F**). However, we found that the combination of PD-1 blockade and MEKi treatment resulted in profound tumor regression in all treated mice (**Fig. 5F**). While these results do not directly implicate roles for TNFα or IFNγ, they nonetheless suggest that immunotherapeutics known to induce their expression can synergize with MEKi in induction of anti-tumor responses.

Enhancement of cell cycle arrest and apoptosis by MEKi and cytokine treatment is broadly evident in lung cancer cells

We showed above that multiple human lung cancer and melanoma cell-lines upregulate TNFR1 expression upon MEKi treatment. We next tested whether cytokine and MEKi effects on viable cell numbers observed in A549 and LKR were generalizable to the additional human lung cancer cell-lines PC-9, H1437, HCC44 and H23. Viable cell numbers were reduced most substantially in the combined presence of TNFα + IFNγ and MEKi **(Fig. 6A)**. Unexpectedly, TNFα and IFNγ did not repress cell numbers in melanoma cell lines **(Fig. 6B)** and cytokines combined with MEKi did not enhance the MEKi inhibitory effect **(Fig. 6B, C).** The combination of cytokines and MEKi synergistically reduced viable cell numbers as determined by the Bliss score in lung cancer lines **(Fig. 6C)**. These results indicate that sensitivity to TNFα + IFNγ and synergy with MEKi occurs in lung but not in melanoma cells. As observed with trametinib, treatment of A549 and HCC44 with additional MEKi and TNFα + IFNγ also significantly reduced viable cell numbers in A549 and HCC44 (**Fig. S9**).

Consistent with above results, cytokines combined with MEKi treatment led to a significant reduction in S-phase cells in the two of the three lung cancer cell lines tested (**Fig. 6D**). We next determined apoptotic sensitivity of these lung cancer cells to MEKi and cytokine treatment. In the highly MEKi sensitive melanoma cell line WM164, a dramatic increase in CC3 generation was evident after 10nM MEKi trametinib treatment (**Fig. 6E**). In contrast, 10nM trametinib induced little CC3 in lung cancer cell lines which was moderately increased by 100nM trametinib. Treatment of lung cancer cells with TNFα + IFNγ also induced little CC3 generation but the combination of cytokines and MEKi dramatically enhanced CC3 levels (**Fig. 6E;** see boxed lanes), consistent with decrease in viable cells seen after this combination treatment (**Fig. 6A**). In these cell lines, the overall CC3 levels rather than specifically the p19 and p17

forms were associated with loss of viable cells. Together with above findings in A549 and LKR, these results indicate that while lung cancer cells are largely resistant to apoptosis induction by MEKi, their apoptotic sensitivity is substantially increased in the presence of TNFα + IFNγ.

Discussion

The studies presented here demonstrate a novel and unexpected link between MEK inhibitors and TNFα signaling in lung cancer cells. We show that the upregulation of cell surface TNFR1 expression is a general and widespread effect of MEK inhibition as it was evident across an array of human and mouse cancer cells from different tumor types and with distinct driver oncogene mutations. The upregulation of TNFR1 not only enhanced TNFα induced responses but also those jointly controlled by TNFα and IFNγ. Crucial amongst them were gene expression, cell cycle arrest and cell death. In multiple human lung cancer cell lines, we show that the combination of cytokines and MEKi induced the highest levels of cell cycle arrest and apoptosis. In vivo studies performed with human A549 showed that TNFR1 deficiency attenuated the MEKi anti-tumor response. Interestingly, TNFα and IFNγ did not induce growth suppression or enhance MEKi-induced growth suppression in melanoma cells. The underlying reason for this difference is not presently clear but may indicate intrinsic resistance of melanoma cells to growth suppression and cell death induction by these cytokines. A recent study showed relatively low trametinib treatment response (12%) in NSCLC with *KRAS* mutations (4). Our results suggest that combining MEKi with agents that promote TNFα and IFNγ expression, such as checkpoint blockade or T cell adoptive cell therapy (ACT), may help achieve greater benefit in lung cancer patients. In this setting, distinct mechanisms may cooperatively promote anti-tumor responses through synergistic increase in expression of immune function genes, and most important, the potentiation of growth suppression and cell death. Furthermore, TNFα and IFNγ expression and/or pathway activation could provide a predictive and prognostic biomarker of MEKi treatment response.

Our results indicate that a crucial aspect of cross-talk between MEKi and TNFα/IFNγ is the augmentation of cell death, which is mediated by caspase-induced apoptosis. At trametinib concentrations achieved in patients (~10-12nM) (32), this agent essentially induced no CC3

activation in lung cancer cells. However, at the same concentrations, trametinib combined with TNFα+IFNγ induced robust CC3 activation coincident with loss of viable cells. In vivo studies indicate that high levels of these cytokines (e.g. by cytokine injection or potentially induced by PD-1 blockade) enhance tumor regression compared to individual treatments. This is consistent with our findings showing a cytokine dose-dependent increase in apoptotic marker CC3 suggesting that synergy between MEKi and cytokines will be enhanced in proportion to cytokine levels. In all lung cancer cell lines tested, we have observed that the combination of MEKi with both TNFα and IFNγ is required for maximal loss of viable cells. However, several aspects of these findings require further investigation: first, in LKR cells, these 2 cytokines had distinct effects on CC3 generation individually and when combined with MEKi. Thus, the contribution of individual cytokines and synergy between them in apoptosis induction with MEKi requires further study in LKR as well as in additional cell types in order to better define underlying mechanisms. Second, we have surmised that increase in TNFα responses through TNFR1 upregulation enhance gene expression, cell cycle arrest and cell death responses jointly regulated by TNFα + IFNγ. However, it remains to be determined whether MEKi also impacts the IFNγ pathway, irrespective of effect on the TNFα pathway. While MEKi did not impact STAT1 activation by IFNγ in A549, it is nonetheless possible that more subtle cross talk exists between MEKi and the IFNγ pathway. Finally, TNFR1 deficiency in A549 led to partial resistance to MEKi. While exogenous cytokine addition universally synergizes with MEKi to reduce lung cancer cell viability, it remains to be determined whether TNFR1 deficiency is also sufficient for conferring resistance to MEKi treatment. The direct systemic administration of TNFα and/or IFNγ is expected to be quite toxic. Type 1 IFN (e.g. IFNα) share many key features with type II IFN (IFNγ), and importantly, IFNα has been in clinical use for cancer treatment for many years. Interestingly, we found that similar to IFNγ, IFNα also synergized with TNFα and MEKi in enhancing gene expression and decreasing cell viability (**Fig. S10A, B**). While this combination

needs to be first tested in preclinical models, if effective, it can be explored in the clinical setting as a novel combination treatment for cancer.

Sensitivity to TNFα induced apoptosis is controlled by the balance of pro-death and pro-survival pathways. NF-κB functions in suppressing both TNFα and IFNγ induced apoptosis and necroptosis cell death pathways (33, 34). However, MEKi enhances NF-κB activation while concomitantly promoting cell death. One possibility is that the magnitude of cell death pathway enhancement by MEKi and cytokines is such that it cannot be controlled by NF-κB pro-survival functions. In human lung cancer cell lines, TNFα and IFNγ cooperatively promoted cell cycle arrest with MEKi. Therefore, loss of viable human lung cancer cells after combined treatment with cytokines and MEKi likely results from both cell cycle arrest and cell death. In contrast, MEKi combined with cytokines did not enhance cell cycle arrest in mouse LKR cells where increase in cell death appears to be the dominant pathway. Previous studies showed that these cytokines synergistically induce cancer cell growth suppression through cell cycle arrest and senescence induction that is mediated by the CDK/Rb pathway (28). While we did not observe a clear cell cycle arrest phenotype in human lung cancer cell lines after treatment with TNFα and IFNγ, it is possible that MEKi induced increase in cytokine signaling enhances growth suppression through the CDK/Rb pathway.

The mechanism by which MEKi may enhance cell surface TNFR1 expression is not clear. Our results indicate that total protein expression of TNFR1 was not impacted by distinct MEKi (**Fig. 3C and S4A**). Consistent with this, we did not detect any substantial change in TNFR1 mRNA expression after MEKi treatment (**Fig.S11**). These results indicate that enhancement of surface expression is not due to increased de novo synthesis but rather increased cell surface localization of TNFR1. While the mechanism by which MEKi may enhance cell surface TNFR1 expression is not clear, a previous study implicated a role for ERK sites in the TNFR1

transmembrane domain in preventing membrane localization (35). To investigate whether MEKi enhances cell surface TNFR1 expression through this mechanism, we mutated two candidate sites (T244A, S278A) in TNFR1 and re-expressed in TNFR1 knockout A549 and PC-9. Although TNFR1 expression varied amongst these cell lines, we did not observe differences in baseline or MEKi-induced membrane expression of wild-type vs. mutated receptors (**Fig. S12**). These results suggest that either individual mutation of these sites is not sufficient to impact membrane localization or that potentially distinct MEKi-induced mechanisms may control TNFR1 surface expression.

One of our key findings is that MEKi-induced upregulation of TNFR1 enhances TNFα-induced NF-κB activation and TNFα target gene expression, including immune surveillance genes such as T cell chemokines that are jointly regulated by TNFα and IFNγ. The increase in IFNγ induced gene expression is likely to be mediated by increase in MEKi induced cell surface TNFR1 expression, which enhances TNFα autocrine signaling and synergy with IFNγ. Our findings suggest that the upregulation of TNFR1 expression may provide a mechanistic explanation for BRAFi/MEKi mediated increase in tumor immunogenicity seen in melanoma patients (11-13). Thus, the increase in NF-κB activity evident after BRAFi/MEKi treatment could be mediated through a greater response to TNFα and IFNγ following increase in TNFR1 expression. Since loss of viable cells was not increased by cytokines and MEKi in melanoma cells, it is possible that the combined immune stimulatory effect of MEKi and cytokines augments anti-tumor activity. Such differential impact of MEKi in melanoma vs. lung tumor models requires further study. Previous studies have implicated the RAL-TBK1 signaling arm of RAS in expression of pro-inflammatory cytokines with tumor-promoting functions (e.g. IL6) (36). Based on our findings, it will also be interesting to determine whether potential cross-talk between TBK1 and/or other oncogenic pathways and TNFα/IFNγ also impacts gene expression and cell death pathways.

Acknowledgements

We thank colleagues from Moffitt Cancer Center Drs. Jae-Young Kim for providing cell-lines, reagents and technical support, and Dr. Jose Conejo-Garcia for thoughtful comments on this manuscript. We thank Dr. Dung-Tsa Chen and Ram Thapa for help with statistical analysis, and Dr. Manali S. Phadke for help with melanoma cell lines. This work was supported by funds from the Moffitt Cancer Center's Miles for Moffitt, Lung Cancer Center of Excellence, Prelude to a Cure, and the DoD Lung Cancer Research Program (Grant # LC140306) (supporting A.A.B), The Moffitt Skin SPORE P50 CA168536 (to A.A.B and K.S.M.S) and a James and Esther King Biomedical Research Program Grant (5JK06) from the Florida Department of Health (supporting N.T.G. and W.D.C.). We would like to acknowledge the Molecular Genomics, Cancer Informatics, Tissue Core, Analytic Microscopy, and Flow Cytometry shared facilities at Moffitt Cancer Center; an NCI designated Comprehensive Cancer Center supported by NIH P30-CA076292.

References

1. Fedorenko IV, Paraiso KH, Smalley KS. Acquired and intrinsic BRAF inhibitor resistance in BRAF V600E mutant melanoma. Biochem Pharmacol. 2011;82:201-9.
2. Zhao Y, Adjei AA. The clinical development of MEK inhibitors. Nature reviews Clinical oncology. 2014;11:385-400.
3. Meador CB, Pao W. Old Habits Die Hard: Addiction of BRAF-Mutant Cancer Cells to MAP Kinase Signaling. Cancer discovery. 2015;5:348-50.
4. Blumenschein GR, Jr., Smit EF, Planchard D, Kim DW, Cadranel J, De Pas T, et al. A randomized phase II study of the MEK1/MEK2 inhibitor trametinib (GSK1120212) compared with docetaxel in KRAS-mutant advanced non-small-cell lung cancer (NSCLC)dagger. Ann Oncol. 2015;26:894-901.
5. Chen PY, Muzumdar MD, Dorans KJ, Robbins R, Bhutkar A, Del Rosario A, et al. Adaptive and Reversible Resistance to Kras Inhibition in Pancreatic Cancer Cells. Cancer Res. 2018;78:985-1002.
6. Muzumdar MD, Chen PY, Dorans KJ, Chung KM, Bhutkar A, Hong E, et al. Survival of pancreatic cancer cells lacking KRAS function. Nat Commun. 2017;8:1090.
7. Singh A, Greninger P, Rhodes D, Koopman L, Violette S, Bardeesy N, et al. A gene expression signature associated with "K-Ras addiction" reveals regulators of EMT and tumor cell survival. Cancer cell. 2009;15:489-500.
8. Engelman JA, Chen L, Tan X, Crosby K, Guimaraes AR, Upadhyay R, et al. Effective use of PI3K and MEK inhibitors to treat mutant Kras G12D and PIK3CA H1047R murine lung cancers. Nature medicine. 2008;14:1351-6.
9. Yuan TL, Amzallag A, Bagni R, Yi M, Afghani S, Burgan W, et al. Differential Effector Engagement by Oncogenic KRAS. Cell Rep. 2018;22:1889-902.
10. Papke B, Der CJ. Drugging RAS: Know the enemy. Science. 2017;355:1158-63.
11. Frederick DT, Piris A, Cogdill AP, Cooper ZA, Lezcano C, Ferrone CR, et al. BRAF inhibition is associated with enhanced melanoma antigen expression and a more favorable tumor microenvironment in patients with metastatic melanoma. Clin Cancer Res. 2013;19:1225-31.
12. Kakavand H, Wilmott JS, Menzies AM, Vilain R, Haydu LE, Yearley JH, et al. PD-L1 Expression and Tumor-Infiltrating Lymphocytes Define Different Subsets of MAPK Inhibitor-Treated Melanoma Patients. Clin Cancer Res. 2015;21:3140-8.
13. Massi D, Brusa D, Merelli B, Falcone C, Xue G, Carobbio A, et al. The status of PD-L1 and tumor-infiltrating immune cells predict resistance and poor prognosis in BRAFi-treated melanoma patients harboring mutant BRAFV600. Ann Oncol. 2015;26:1980-7.
14. Gajewski TF, Schreiber H, Fu YX. Innate and adaptive immune cells in the tumor microenvironment. Nat Immunol. 2013;14:1014-22.
15. Herbst RS, Soria JC, Kowanetz M, Fine GD, Hamid O, Gordon MS, et al. Predictive correlates of response to the anti-PD-L1 antibody MPDL3280A in cancer patients. Nature. 2014;515:563-7.
16. Tumeh PC, Harview CL, Yearley JH, Shintaku IP, Taylor EJ, Robert L, et al. PD-1 blockade induces responses by inhibiting adaptive immune resistance. Nature. 2014;515:568-71.
17. Cooper ZA, Juneja VR, Sage PT, Frederick DT, Piris A, Mitra D, et al. Response to BRAF inhibition in melanoma is enhanced when combined with immune checkpoint blockade. Cancer immunology research. 2014;2:643-54.
18. Ho PC, Meeth KM, Tsui YC, Srivastava B, Bosenberg MW, Kaech SM. Immune-based antitumor effects of BRAF inhibitors rely on signaling by CD40L and IFNgamma. Cancer Res. 2014;74:3205-17.
19. Hu-Lieskovan S, Mok S, Homet Moreno B, Tsoi J, Robert L, Goedert L, et al. Improved antitumor activity of immunotherapy with BRAF and MEK inhibitors in BRAF(V600E) melanoma. Science translational medicine. 2015;7:279ra41.

20. Ebert PJR, Cheung J, Yang Y, McNamara E, Hong R, Moskalenko M, et al. MAP Kinase Inhibition Promotes T Cell and Anti-tumor Activity in Combination with PD-L1 Checkpoint Blockade. Immunity. 2016;44:609-21.
21. Hopewell EL, Zhao W, Fulp WJ, Bronk CC, Lopez AS, Massengill M, et al. Lung tumor NF-kappaB signaling promotes T cell-mediated immune surveillance. J Clin Invest. 2013;123:2509-22.
22. Kwong LN, Boland GM, Frederick DT, Helms TL, Akid AT, Miller JP, et al. Co-clinical assessment identifies patterns of BRAF inhibitor resistance in melanoma. J Clin Invest. 2015;125:1459-70.
23. Ueda Y, Richmond A. NF-kappaB activation in melanoma. Pigment Cell Res. 2006;19:112-24.
24. Xia Y, Shen S, Verma IM. NF-kappaB, an active player in human cancers. Cancer immunology research. 2014;2:823-30.
25. Wilmott JS, Haydu LE, Menzies AM, Lum T, Hyman J, Thompson JF, et al. Dynamics of chemokine, cytokine, and growth factor serum levels in BRAF-mutant melanoma patients during BRAF inhibitor treatment. J Immunol. 2014;192:2505-13.
26. Bai Y, Kim JY, Watters JM, Fang B, Kinose F, Song L, et al. Adaptive responses to dasatinib-treated lung squamous cell cancer cells harboring DDR2 mutations. Cancer Res. 2014;74:7217-28.
27. Derakhshan A, Chen Z, Van Waes C. Therapeutic Small Molecules Target Inhibitor of Apoptosis Proteins in Cancers with Deregulation of Extrinsic and Intrinsic Cell Death Pathways. Clin Cancer Res. 2017;23:1379-87.
28. Braumuller H, Wieder T, Brenner E, Assmann S, Hahn M, Alkhaled M, et al. T-helper-1-cell cytokines drive cancer into senescence. Nature. 2013;494:361-5.
29. Suk K, Chang I, Kim YH, Kim S, Kim JY, Kim H, et al. Interferon gamma (IFNgamma) and tumor necrosis factor alpha synergism in ME-180 cervical cancer cell apoptosis and necrosis. IFNgamma inhibits cytoprotective NF-kappa B through STAT1/IRF-1 pathways. J Biol Chem. 2001;276:13153-9.
30. Zheng H, Zhao W, Yan C, Watson CC, Messengill M, Xie M, et al. HDAC inhibitors enhance T cell chemokine expression and augment response to PD-1 immunotherapy in lung adenocarcinoma. Clin Cancer Res. 2016;22:4119-32.
31. Wei F, Zhong S, Ma Z, Kong H, Medvec A, Ahmed R, et al. Strength of PD-1 signaling differentially affects T-cell effector functions. Proc Natl Acad Sci U S A. 2013;110:E2480-9.
32. Kim KB, Kefford R, Pavlick AC, Infante JR, Ribas A, Sosman JA, et al. Phase II study of the MEK1/MEK2 inhibitor Trametinib in patients with metastatic BRAF-mutant cutaneous melanoma previously treated with or without a BRAF inhibitor. J Clin Oncol. 2013;31:482-9.
33. Beg AA, Baltimore D. An essential role for NF-kappaB in preventing TNF-alpha-induced cell death. Science. 1996;274:782-4.
34. Thapa RJ, Basagoudanavar SH, Nogusa S, Irrinki K, Mallilankaraman K, Slifker MJ, et al. NF-kappaB protects cells from gamma interferon-induced RIP1-dependent necroptosis. Mol Cell Biol. 2011;31:2934-46.
35. Van Linden AA, Cottin V, Leu C, Riches DW. Phosphorylation of the membrane proximal region of tumor necrosis factor receptor CD120a (p55) at ERK consensus sites. J Biol Chem. 2000;275:6996-7003.
36. Zhu Z, Aref AR, Cohoon TJ, Barbie TU, Imamura Y, Yang S, et al. Inhibition of KRAS-driven tumorigenicity by interruption of an autocrine cytokine circuit. Cancer discovery. 2014;4:452-65.

Figure Legends

Fig. 1 MEK inhibitors enhance TNFα induced gene expression. (A) NF-κB signature activity in paired melanoma patient biopsies at pre-treatment (pre) and under vemurafenib or dabrafenib plus trametinib treatment (on). Individual lines represents each pair of biopsies, anonymized patient ID along with the tumor reduction rate (%). (B) Correlation between individual patient response (% tumor reduction) to treatment and NF-κB signature score in on-treatment biopsies. Red line represents Pearson's linear correlation. (C-D) Time course expression of *TNF* and *TNFAIP3* mRNA in WM164 and 1205Lu as indicated. Cells were incubated with trametinib (TRA, 10nM) or left unstimulated for 24 hours, with or without 2ng/ml TNFα added for indicated time periods. 0h on the x-axis indicates no treatment (black circle) or TRA alone treatment for 24 hours (red circle). Gene expression was determined in triplicate samples by qPCR and normalized to unstimulated cells. Two-way ANOVA was used to determine significance of difference between single and combined treatments (indicated on top). A *post hoc* Sidak's multiple-comparison test for each time point was also performed and is overlaid on the plot at specific time points. *p<0.05, **p<0.01, ***p<0.001. NS: not significant. (E) Microarray expression of select TNFα target genes in A549 subjected to indicated treatments; TRA treatment was 24 hours, TNFα was 2 hours. Expression value is represented using a z-score range of 3 standard deviations from the mean. (F) Time course expression of *TNF* and *TNFAIP3* mRNA in A549 as described in C. (G) Time course expression of *CXCL10* in A549, cells were incubated with TRA for 24 hours or left unstimulated, with or without 2ng/ml cytokines (TNFα, IFNγ) added for indicated time period. Two-way ANOVA was used to determine significance of difference with and without presence of TRA in indicated groups. P*ost hoc* Sidak's multiple-comparison test was performed and is overlaid on the plot for the TNFα + IFNγ and TNFα + IFNγ + TRA group comparison. *p<0.05, **p<0.01, ***p<0.001. NS: not significant. (H) A549 supernatants were collected from A549 cells subjected to indicated treatments,

CXCL10 secretion were determined using the Luminex assay. Data represents the mean ± SD. Significances were determined using one-way ANOVA and a *post hoc* Sidak's multiple-comparison test. *p<0.05, **p<0.01, ***p<0.001. NS: not significant.

Fig. 2 MEK and ERK inhibitors stimulate TNFα + IFNγ induced chemokine expression.

(A) Outline of drug screening assay used to identify agents that enhance TNFα and IFNγ induced expression of CXCL10 and/or CCL5 2-fold over cytokines alone. TNFα and IFNγ were added to final concentrations of 0.2 ng/ml and 1 ng/ml, respectively. Library compounds were used at 0.1 μM or 1 μM. (B) Agents that enhance TNFα and IFNγ induced expression of CXCL10 and/or CCL5 2-fold over cytokines alone in at least one of the four tested conditions are indicated. Drug target categories are also indicated (see results for details). Arry162 (aka MEK162, binimetinib), a MEKi, induced 1.9-fold increase was also added to show similarity to other MEKi and is indicated with an *. Certain drugs were used in duplicate (LC-161; shown as 1 and 2) to test reproducibility of results.

Fig. 3. MEKi enhance cell surface expression of TNFα receptor 1. (A) Cell surface TNF receptor 1 (TNFR1) expression in A549 was examined by flow cytometry after 24 hours trametinib (TRA) treatment at 1nM, 10nM and 100nM. US, unstained; UT, untreated. (B) A549 cell surface expression of TNFR1 and TNFR2 was quantified based on median florescence intensity (MFI). (C) Total cell lysates were prepared to perform western blots to detect ERK and TNFR1 in A549 after indicated treatments. (D) Western Blot showing RelA phosphorylation (serine 536; p-RelA) and overall nuclear levels of RelA (p65) in A549 that were subjected to indicated treatments, total incubation time of TRA was 24 hours and cytokines were added in the last 6 hours. Concentrations: TRA 100nM, IFNγ 50ng/ml, TNFα 25ng/ml. ERK and β-actin levels are also shown. (E) Cell surface TNFR1 expression fold change in indicated cell lines upon 24 hours 100nM TRA treatment. Plot represents mean ± SD of 3 replicates. Sidak's

correction for multiple t-test were applied to determine significance of the change in each cell line. (F) Kras-G12D was expressed in NIH-3T3 cells using pBABE-Kras retrovirus. Western blots showing ERK and β-actin in NIH-3T3 cells. (G) Cell surface TNFR1 expression after indicated treatments was determined in NIH-3T3 cells described in F. Plot represents mean ± SD of 3 replicates, Sidak's multiple-comparison for t-test were applied to determine significance of the changes. ****p<0.0001 (H) TNFR1 expression in A549 was knocked out (TNFR1KO) using CRISPR/Cas9 technology. To re-express TNFR1 in TNFR1KO A549, cells were infected by pLPC-TNFR1 or pLPC retrovirus. *CXCL10* mRNA expression was determined by qPCR after indicated treatments, gene expression levels were normalized to unstimulated cells. Concentrations: TRA 100nM, IFNγ 50ng/ml, TNFα 25ng/ml. Data represent the mean ± SD of triplicate values. Two-way ANOVA and a *post hoc* Tukey's multiple-comparison test was performed for the TNFα + IFNγ and TNFα + IFNγ + TRA group comparison as indicated. *p<0.05, **p<0.01, ***p<0.001. NS: not significant.

Fig. 4 TNFα and IFNγ enhance MEKi induced growth suppression and cell death. (A) In vitro MEKi sensitivity of A549. TNFR1 was re-expressed in TNFR1KO-A549 using pLPC-TNFR1 retrovirus (TNFR1KO-TNFR1), pLPC used as control (TNFR1KO-pLPC). 10^4 of A549, TNFR1KO, TNFR1KO-TNFR1 and TNFR1KO-pLPC were seeded into 6 well plates, and incubated with 1nM TRA or left untreated for the next 4 days, viable cell numbers were counted at day 4 for each cell line and normalized to untreated. (B) Impact of TRA and cytokines on A549 growth in vitro. 3 X 10^4 cells were seeded into 6 well plates and incubated with 10nM TRA with or without 2ng/ml each cytokine (TNFα, IFNγ) for the next 4 days, viable cell numbers were counted on day 4 and normalized to untreated (UT). Plot represents mean ± SD of 3 replicates, significance was determined using one-way ANOVA and a *post hoc* Tukey's multiple-comparison test and is shown for indicated comparisons. ****p < 0.0001. (C) Cell cycle analysis of A549 after treatments indicated, cells were collected at day 2 after treatments. Propidium

Iodide (PI) staining was used to determine percentage of cells in different cell cycle stages as indicated. Comparisons were made using a chi-squared test with Bonferroni correction. Plot shows representative result from 3 independent experiments, complete results can be found in Table S3. (D) Western blot showing apoptosis marker cleaved caspase 3 expression in A549 after 48 hours of indicated treatment. Cytokines concentration was at 2ng/ml. (E) Trametinib (TRA) effect on growth of lung orthotopic A549 tumors (WT) and TNFR1KO A549 tumors in immunodeficient SCID mice. After 14 days of tumor cell inoculation, 1mg/kg TRA or vehicle was administrated daily through oral gavage for 14 days. UT indicates vehicle treated mice. At the end of treatment, lungs were collected from viable mice for H&E staining. Tumor percentage was quantified based on tumor tissue area compared to total lung area (%). (F) H&E staining of paraffin sections described in E. (G) p-ERK IHC staining in TNFR1KO A549 tumors (untreated and 1mg/kg TRA treated) from E.

Fig. 5 TNFα and IFNγ synergize with MEKi to induce lung cancer cell death. (A) Impact of TRA and cytokines on LKR growth in vitro was determined as in Fig. 4B except treatment was for 2 days. Plot represents mean ± SD of 3 replicates, significance was determined using one-way ANOVA and a *post hoc* Tukey's multiple-comparison test and is shown for indicated comparisons. ** $p<0.01$, *** $p<0.001$ ****, $p < 0.0001$ (B) Cell cycle analysis of LKR after treatments indicated was performed as in Fig.4C. Comparisons were made using a chi-squared test with Bonferroni correction of S versus G1/G2 frequencies. Plot shows representative result from 3 independent experiments, complete results can be found in Table S3. (C) Western blot showing apoptosis marker cleaved caspase 3(CC3) in LKR cells after 48 hours of indicated treatments. (D) Western blot showing cleaved caspase 3(CC3) p19 and p17 fragments in LKR cells in response to indicated cytokine concentrations and trametinib after 48 hours treatments. Viable cell number was also determined and is indicated. (E) Impact of continuous TRA and 3 consecutive intratumoral injections of TNFα/IFNγ on growth of subcutaneous LKR tumors.

Experiment scheme is shown, bioluminescence imaging was taken at day 11 and day 14. Total flux of photons of individual mice was calculated and normalized to value at beginning of treatment. Mean ± SD are overlaid as error bars. One-way ANOVA and a *post hoc* Dunnett's multiple-comparison test was performed. (F) TRA and anti-PD-1 antibody (αPD-1) effect on growth of subcutaneous LKR tumors in 129/sv mice using the indicated treatment scheme. Plot showing tumor volume change from baseline at the experiment endpoint (14 days of TRA treatment). Tumor volumes were measured and calculated based on length x length x width/2, and normalized to volume at the beginning of treatment (day 0). Change of -100% indicates complete tumor rejection. Significance was determined using One-way ANOVA and a *post hoc* Dunnett's multiple-comparison test. *p<0.05, **p<0.01, ***p<0.001, ****p<0.001. ns: not significant.

Fig. 6 Enhancement of cell cycle arrest and apoptosis by MEKi and cytokine treatment is broadly evident in lung cancer cells. (A-B) Cell proliferation of human lung cancer cell lines A549, HCC44, H1437, PC-9, H23 (A) and melanoma cell lines 1205Lu, WM164, WM9, WM793 (B) after indicated treatments as in Fig 4B except for only combined presence of TNFα + IFNγ is shown. Cell numbers were counted on day 4 for each cell-line and normalized to untreated cells. (C) Synergy between TRA and cytokines were measured using Bliss score, heatmap showing selected cell lines used in Fig. 6A after indicated treatments. (D) Cell cycle analysis of PC9, HCC44, H23 after treatments indicated, as in Fig.4C. Comparisons were made using a chi-squared test with Bonferroni correction of S versus G1/G2 frequencies. Plot shows representative result from 3 independent experiments, full results can be found in Table S3. (E) Western blot showing comparison between apoptosis induced by TRA plus cytokines in lung cancer cell lines and TRA induced apoptosis in melanoma cell line WM164. Single treatment with TRA and cytokines in lung cancer lines is indicated in blue rectangles and combined treatment in red rectangles.

Figure 1

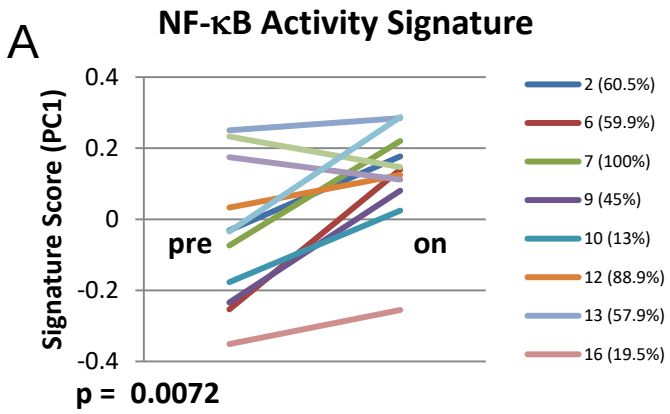

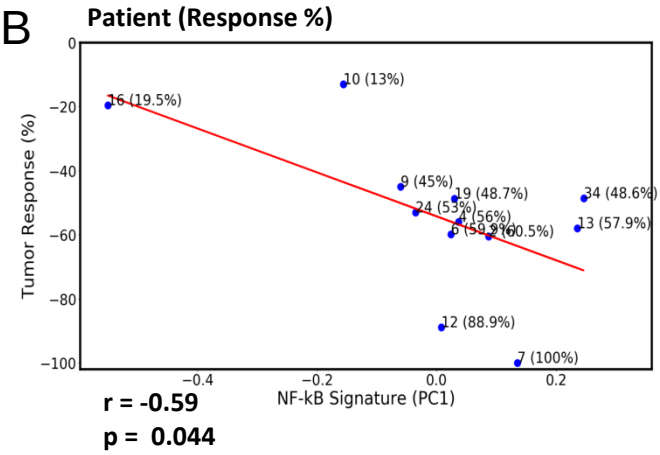

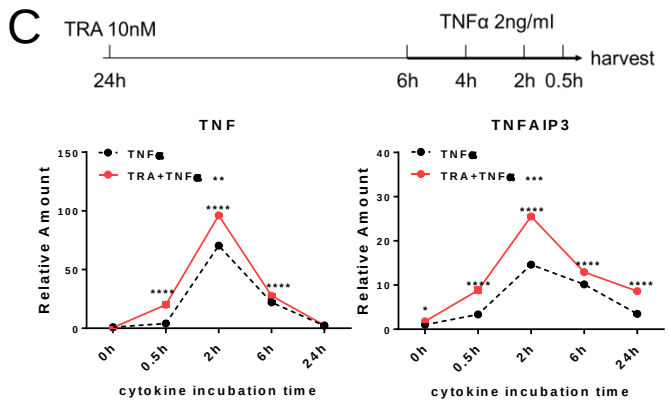

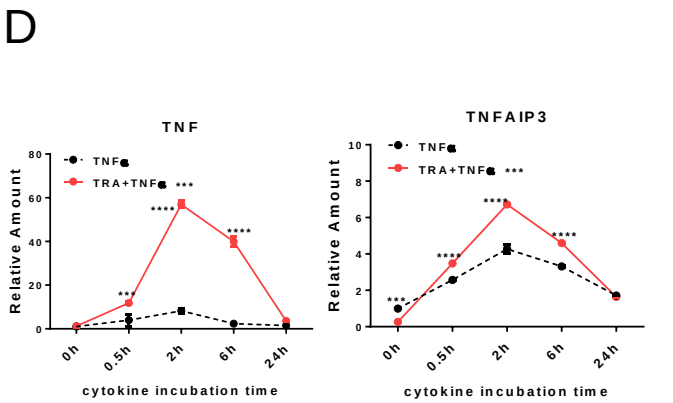

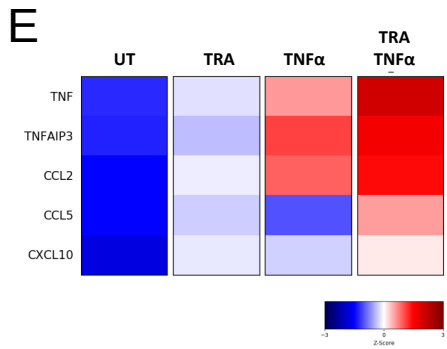

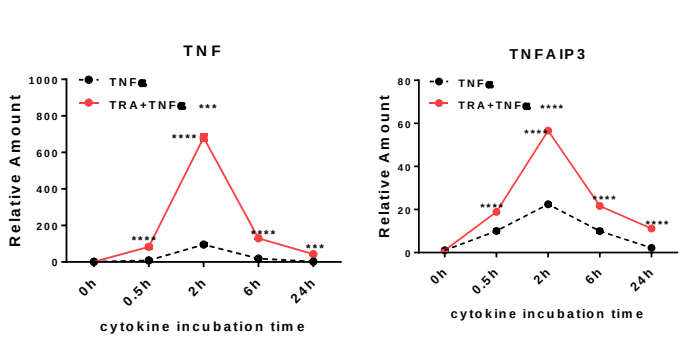

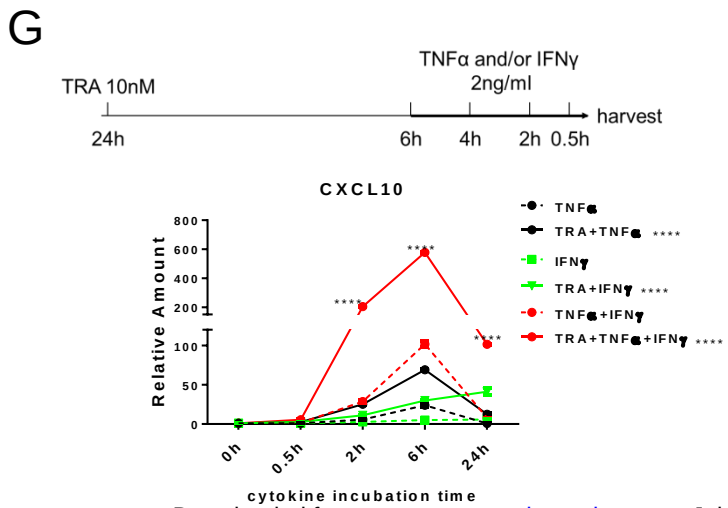

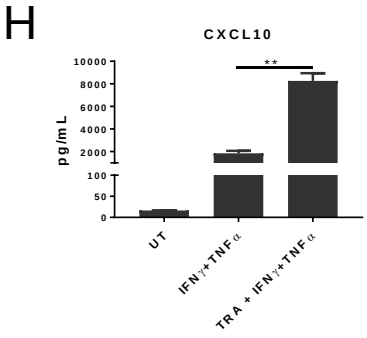

Figure 2

A

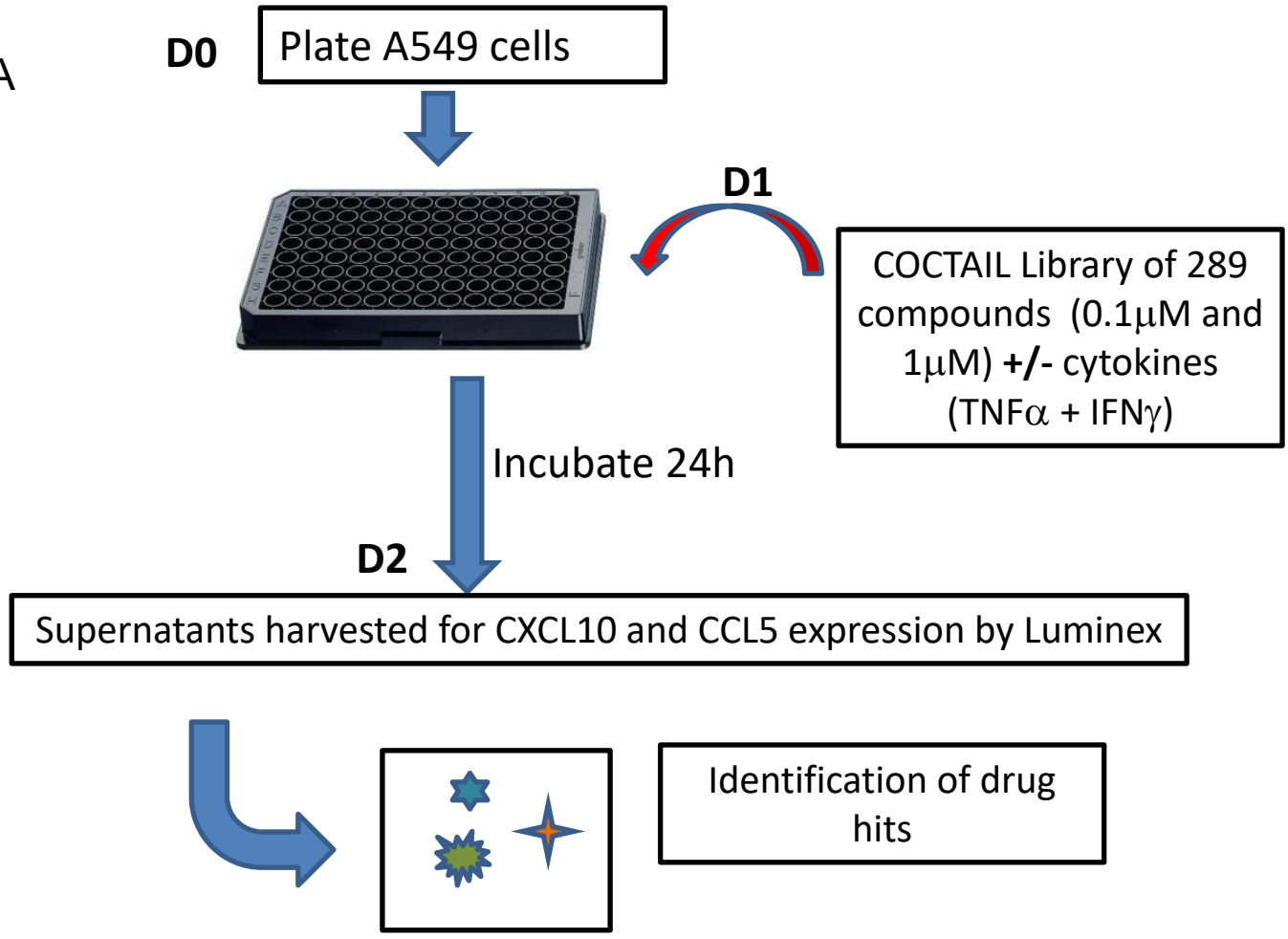

B

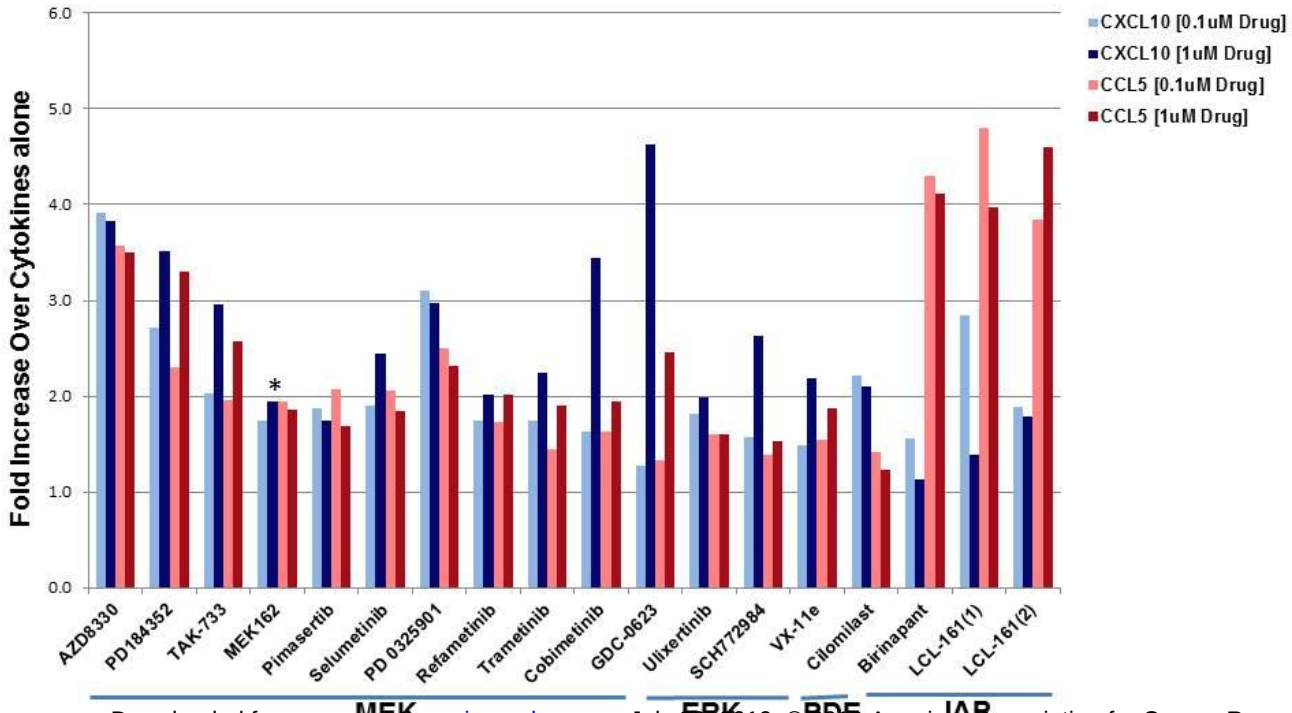

Figure 3

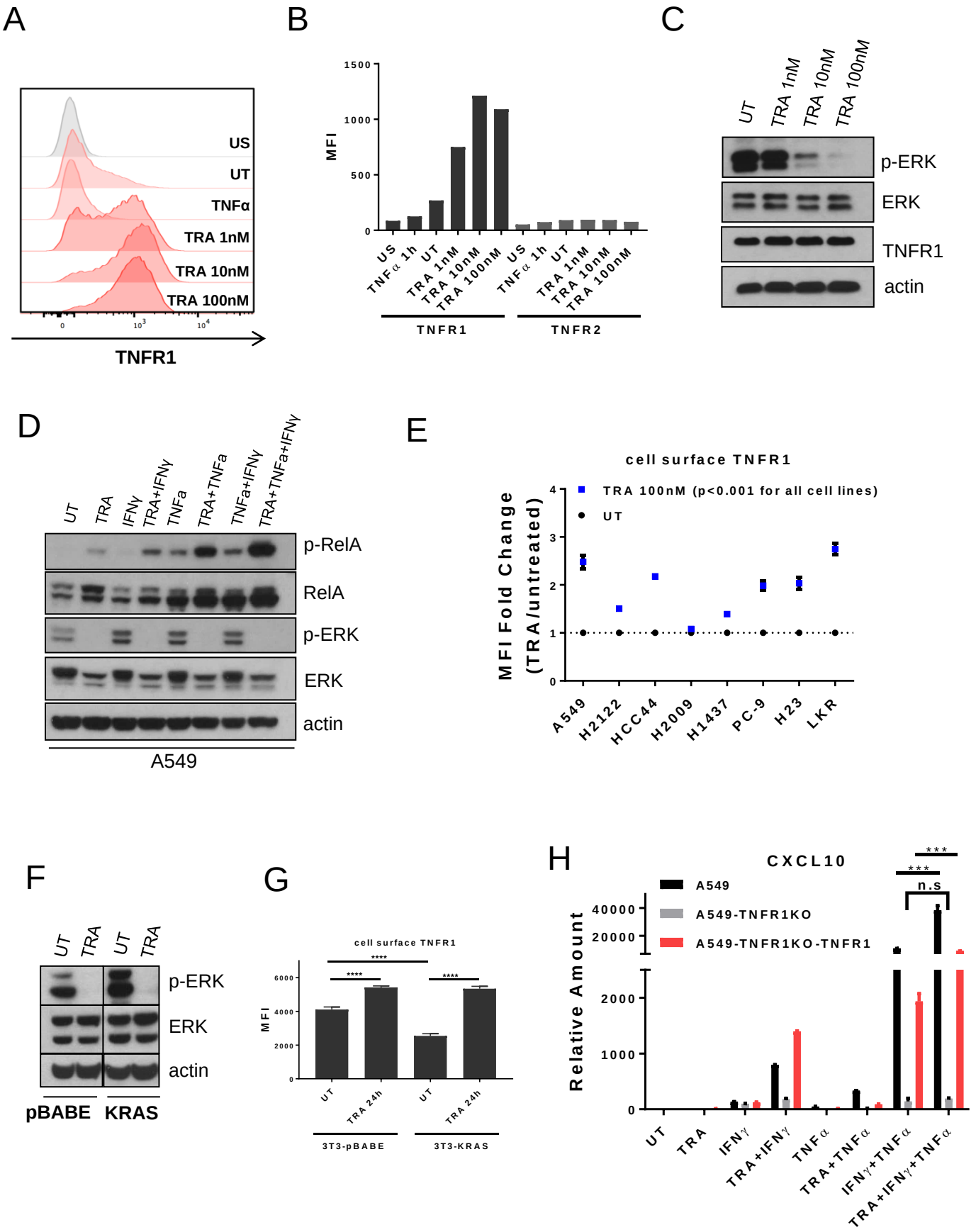

Figure 4

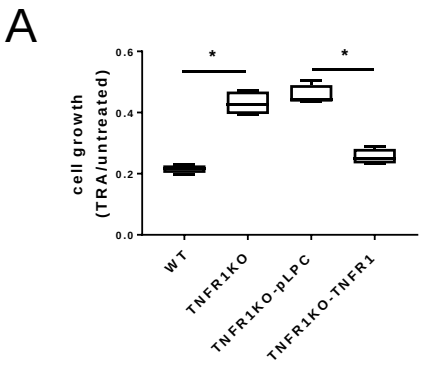

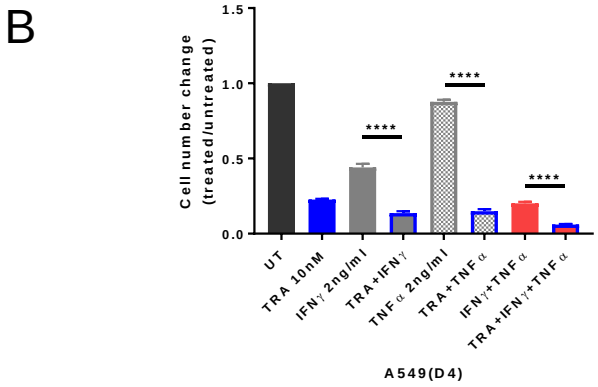

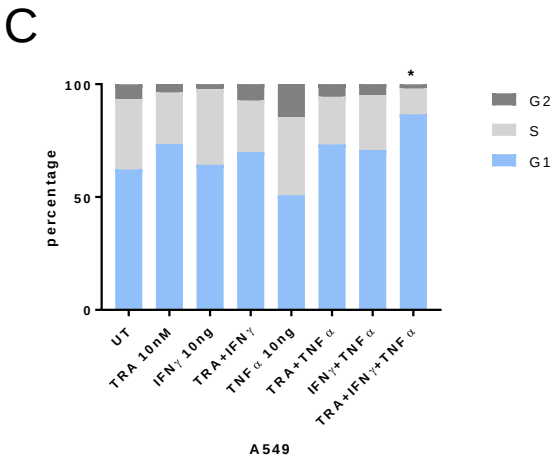

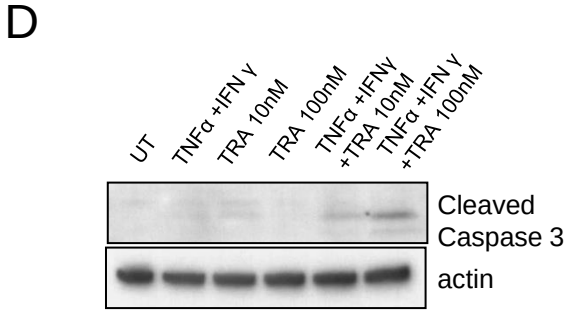

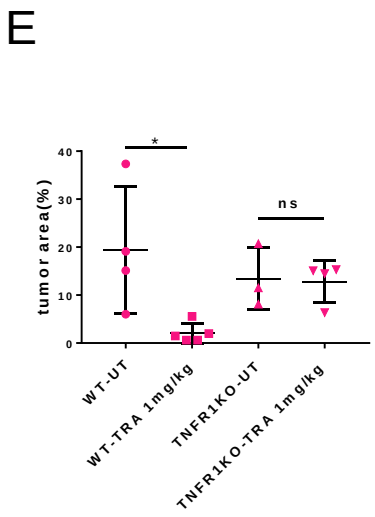

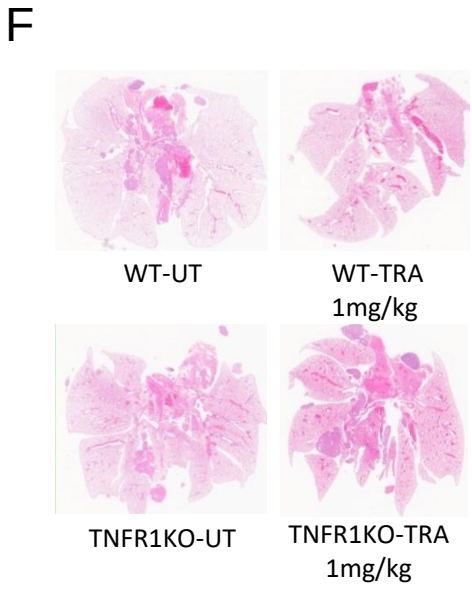

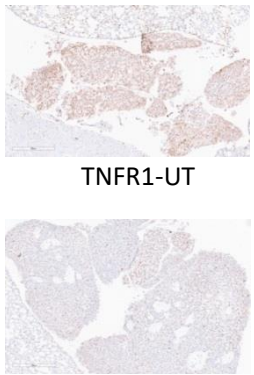

Figure 5

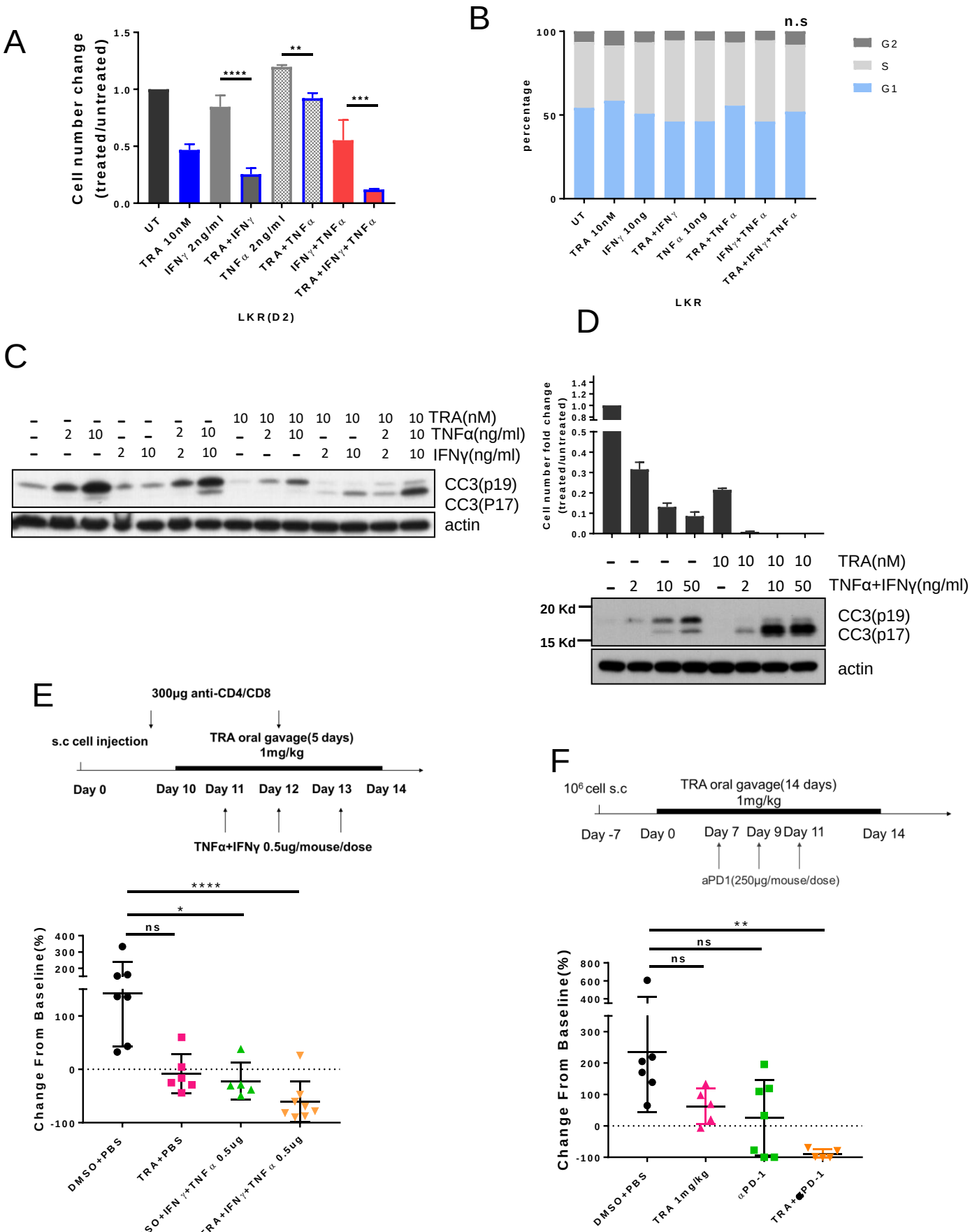

Figure 6

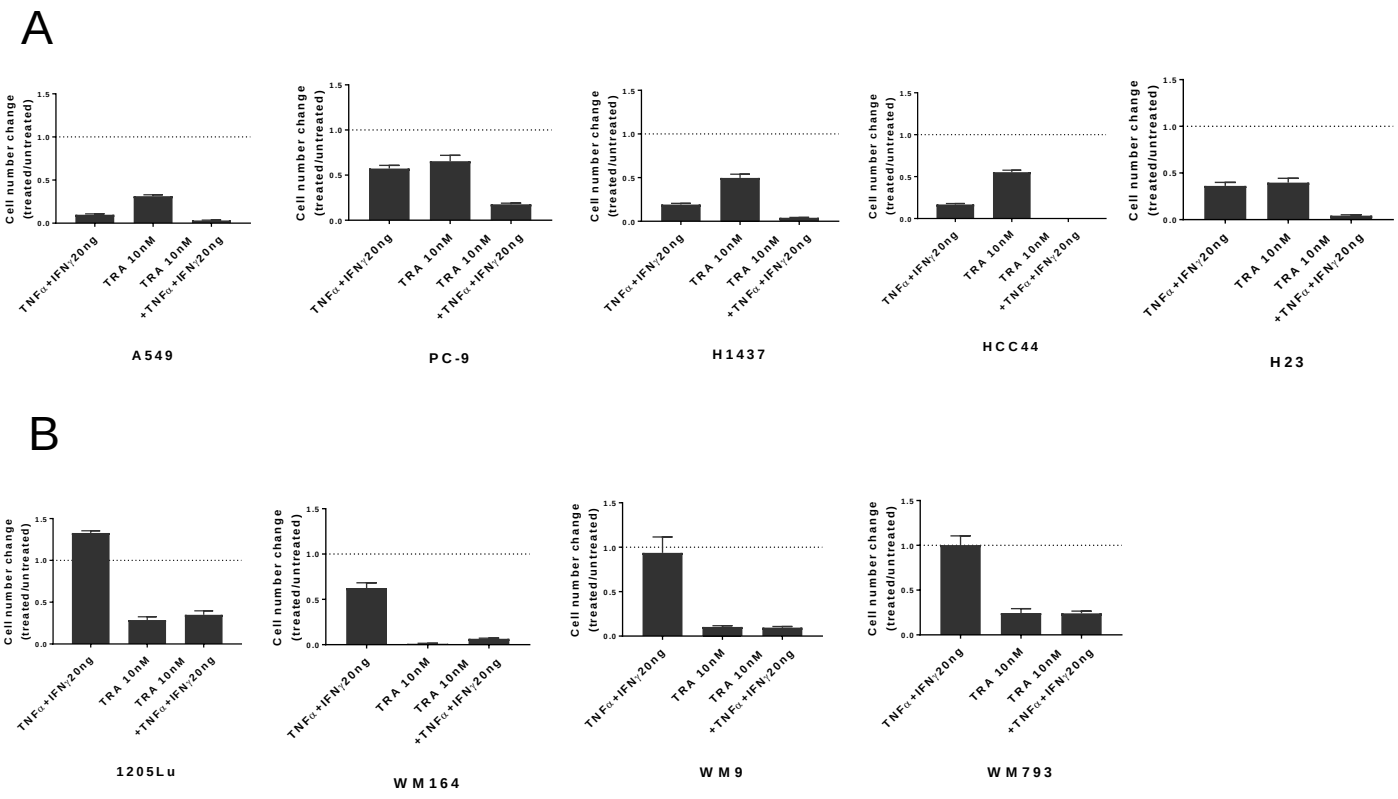

Cancer Research
The Journal of Cancer Research (1916–1930) | The American Journal of Cancer (1931–1940)

AACR American Association for Cancer Research

MEK inhibition modulates cytokine response to mediate therapeutic efficacy in lung cancer

Mengyu Xie, Hong Zheng, Ranjna Madan-Lala, et al.

Cancer Res Published OnlineFirst July 30, 2019.